Accurate Motion Controller Design Based on an Extended Pole Placement Method and a Disturbance Observer

Hendrik Van Brussel (1), Chwan-Hsen Chen, Jan Swevers*
Katholieke Universiteit Leuven, Department of Mechanical Engineering, Celestijnenlaan 300 B, 3001 Heverlee, Belgium
* Senior Research Assistant with the N.F.W.O. (Belgian National Fund for Scientific Research)
Received on January 14, 1994

Abstract
The paper describes an innovative integrated design method for accurate tracking in motion control applications, in the presence of external disturbances like friction, cutting forces, etc.
First, an extended pole placement method is developed to design feedforward controllers for applications with known future input commands, like in feeddrives for machine tools. It results in a noncausal reference model with a low-pass characteristic with selectable bandwidth and zero phase shift. A new feedback design approach, based on a state and disturbance observer is introduced. A loop transfer recovery procedure tunes the observer gains to compromise optimally between performance and robustness.
Keywords: Automation, Continuous path control, Algorithms

1 Introduction

The complex shapes involved in modern product designs and the ever increasing pressure for higher productivity call for a drastic improvement of the dynamic behaviour of the motion control systems in future production machinery. The complex workpiece surfaces, generated by CAD-systems, are to be transformed, as accurately as possible, into toolpaths for machine tools or into end effector trajectories for industrial robots. The more discontinuous these tool paths are and the higher the machining speed requirements, the higher the acceleration requirements are on the motion control systems and the more difficult the required tracking accuracies to be met. With the advent of new production processes, like energy beam machining, the normally used tricks, like slowing down at sharp corners, are not acceptable due to the danger of overburning.

Traditional PID-controllers have to compromise between good positioning behaviour and high tracking accuracy. They completely ignore the dynamic effects resulting from fast varying reference commands and therefore they are unsuitable for high-speed contouring and cornering applications.

Two main functions can be distinguished in a motion control system: feedforward and feedback. Feedforward makes the controlled system (as much as possible) equal to the desired system, thereby using future information. An ideal feedforward makes the system output position follow exactly the input reference command. Feedback control utilizes the measured position information to make the output motion equal to the desired motion, in spite of the presence of modelling errors and external disturbances.

In this paper, a novel integrated motion controller design methodology is developed, featuring an innovative feedforward controller and a robust feedback controller based on a disturbance observer.

Rapidly varying reference commands make the use of feedforward information indispensible for reducing tracking errors. The importance of using future commands to enhance servo performance has long been recognized [13]. Existing methods like General Predictive Control (GPC) [4], and cross-coupled control [9] also implicitly incorporate feedforward control. In this paper, a so called extended pole placement method is developed to design servo feedforward controllers for applications with known future commands, like in feeddrives for machine tools. It results in a noncausal reference model with a low-pass characteristic with selectable bandwidth but zero phase shift. It uses a finite-impulse-response (FIR) filter for its uniform frequency response and zero phase errors. By this method, the resulting output motion resembles almost perfectly the command input. Zero phase shift is important for coordinated motion along multiple axes. Also important is that it provides a feedforward input with selectable bandwidth, important in order not to excite hidden system resonances, a feature which existing algorithms ignore.

In motion control systems, integral feedback control is the prevailing method to remove steady-state positioning errors and to cancel out the influence of external disturbances. It however deteriorates system response and incurs instability. Disturbance observers are regarded as a promising prospective substitute for integral control. What is lacking, however, is a systematic design method, for systems with more states than output measurements, that results in a design achieving a balance between robustness and performance. The new feedback design approach, presented in this paper, is based on the Kalman filter concept, which expresses uncertainties in the mathematical model and the measurements in terms of their covariance values. However, instead of having to determine explicitly numerical values for the covariances, the problem is approached from the side of robustness considerations, represented by the maximum singular value of the system loop transfer function. A dynamic model for the disturbance is presumed and the Doyle-Stein loop transfer recovery (LTR) procedure is applied to tune the disturbance observer gain for optimal system robustness. Without sacrificing response bandwidth, the low-frequency disturbance rejection can be significantly improved, with a performance that integral control can hardly compete with.

These two new approaches result in an innovative controller design methodology. Besides the feedforward and the feedback parts, the control structure also contains a reference state generator, which also has an observer-like structure. The resulting controller has a high performance. Although the potential of the resulting controller can already be seen from the example of a machine tool slide, given here, its merits can be fully appreciated when designing controllers for high-order systems, like motion control systems with structural flexibility (e.g. robots, high-bandwidth machine tool feeddrives).

2 Feedforward design: the extended pole placement (EPP) method

Consider a motion control system, with a structure indicated in figure 1, subject to a reference input trajectory y_{ref} and producing an output trajectory y. The control input to the system is u; the discrete transfer function of the open-loop system, relating u to y is given by

$$H(z) = \frac{B(z)}{A(z)}. \qquad (1)$$

Numerator $B(z)$ can be factorized as

$$B(z) = B^+(z)B^-(z) = B^+(z)B^-_{NMP}(z)B^-_{MP}(z),$$

where $B^-(z)$ includes the so called uncancellable zeros, i.e. those outside the unit circle, also called the nonminimum-phase zeros

($B^-_{NMP}(z)$) and the very lightly damped zeros ($B^-_{MP}(z)$).

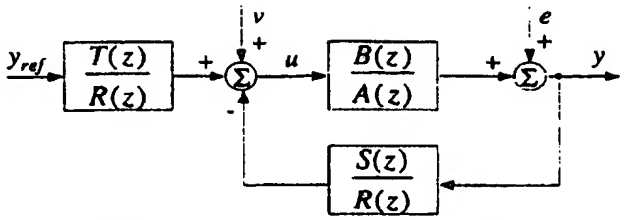

Figure 1: Structure of the controlled system

A servo controller, designed according to the pole placement method, generates a control input according to the following control law:

$$R(z)u(k) = T(z)y_{ref}(k) - S(z)y(k). \quad (2)$$

The desired closed-loop transfer function, which is called the "reference model", is given by:

$$\frac{y(k)}{y_{ref}(k)} = H_{ref}(z) = \frac{B_m(z)}{A_m(z)}. \quad (3)$$

Combining equations (1)-(3) yields:

$$y(k) = \frac{B_m(z)}{A_m(z)}y_{ref}(k) = \frac{B(z)T(z)}{A(z)R(z) + B(z)S(z)}y_{ref}(k). \quad (4)$$

The feedforward function $T(z)$ determines the servo performance of the closed- loop system defined by reference model H_{ref}. After completing the feedback design, H_{ref} simplifies to [2]:

$$H_{ref}(z) = \frac{B^-(z)T(z)}{A_o(z)A_m(z)}, \quad (5)$$

where $A_o(z)$ represents a low-pass filter to trade off between closed-loop performance and noise sensitivity [2]. Remark that $H_{ref}(z)$ contains $B^-(z)$ in its numerator.
The ideal reference model is, of course, $H_{ref} = 1$, in which case there is no distortion nor phase shift between y_{ref} and y. This requirement would yield the following feedforward function:

$$T(z) = \frac{A_o(z)A_m(z)}{B^-(z)}. \quad (6)$$

If $B^-(z)$ contains nonminimum-phase (NMP) zeros, gathered in a factor $B^-_{NMP}(z)$, the feedforward function $T(z)$ becomes unstable.

To solve the problem of the unstable feedforward function $T(z)$, we propose to approximate $1/B^-_{NMP}$ by its truncated Taylor series expansion.

For example, when $B^-_{NMP} = (z-a)/(1-a)$ and $|a| > 1$, $1/B^-_{NMP}$ is approximated by the series

$$\frac{1}{B^-_{NMP}} \approx \frac{a-1}{a^{m+1}-1}\sum_{i=0}^{m} z^i a^{m-i} \equiv \overline{B}^-_{NMP}. \quad (7)$$

Except for zeros very close to the unit circle, a few polynomial terms in Eq. 7 are sufficient to give an accurate approximation to $1/B^-_{NMP}$. Since Eq. 7 contains polynomial terms with positive indices, the resulting feedforward transfer function is always stable.

2.1 Noncausal finite-impulse-response filter

The feedforward function $T(z)$ includes the MP zero factor B^-_{MP} of B^- in order to directly cancel the open-loop transfer function zeros. Including B^-_{MP} in the denominator of $T(z)$ can give violent feedforward signals when the zeros in B^-_{MP} are close to $z = -1$. Since most closed-loop systems behave like a low-pass filter, violent feedforward signals can also result from the fact that their inverse models would greatly amplify the high frequency spectral contents in the commands. This side effect can be remedied by extending Eq. 6 with a noncausal windowed low-pass FIR filter, which attenuates the feedforward function gain at high frequencies without any phase lag:

$$\overline{H}_{FIR}(z) = \sum_{i=0}^{\frac{n_f-1}{2}} w_i h_i (z^i + z^{-i}). \quad (8)$$

w_i is a Hamming window like function and suppresses the ripples of the high order FIR filter near to the cutt-off frequency. This filter has zero phase angle because the phase lead generated by z^i compensates the phase lag generated by z^{-i}. This noncausal filter can be used in most applications where future reference commands are available.

The complete feedforward transfer function $T(z)$, expressed in Eq. 6, now becomes:

$$T(z) = \frac{A_o A_m}{B^-_{MP}}\overline{B}^-_{NMP}\overline{H}_{FIR}, \quad (9)$$

in which $B^-_{MP}/\overline{B}^-_{NMP}$ is an approximation of $1/B^-$, and $\overline{H}_{FIR}$ is added in order to attenuate the high frequency gain of the feedforward controller. The actual control algorithm implemented in the digital computer can be obtained by substituting Eq. 9 into Eq. 2.

2.2 Experimental verification

The experimental test setup is a ballscrew-driven machine tool slide. Its experimentally identified discrete-time transfer function is:

$$H(z) = \frac{1.816 \times 10^{-3}(z + 0.9599)}{(z-1)(z-0.8842)} = \frac{B^+(z)B^-(z)}{A(z)}.$$

It describes the relation between the input $u(k)$, in digital-to-analog converter units, and the encoder output $y(k)$ for a sampling frequency of $250Hz$. The pitch of the ballscrew is 10 mm/rev, and the encoder resolution is 400 counts/rev. Together, they make a basic length unit (BLU) of 0.025 mm.

The required closed-loop response is specified by the characteristic polynomial $A_m(z) = z^2 - 1.2589z + 0.4604$, which is equivalent to a closed-loop bandwidth of 21.68 Hz and a damping ratio ζ of 0.712. These poles are determined using optimal feedback control (see further), which uses weighting between the control effort and the output error.

The feedback function $R(z)$ includes an integrator in order to have high low frequency servo stiffness. The uncancellable, but stable, zero at $z = -0.9599$, is included in $B^-_{MP}(z) = 1.816 \times 10^{-3}(z + 0.9599)$. $B^+(z) = 1$.

Based on the traditional pole placement feedback design procedure (see e.g. [2] for details), thereby trying to maximize the disturbance rejection ability, while keeping the noise response transfer function, relating the measurement noise $e(k)$ to the output $y(k)$ below unity at frequencies above the closed-loop bandwidth, following polynomials result:

$$\begin{aligned} R(z) &= z^2 - 1.323z + 0.323 \\ S(z) &= 69.143z^2 - 125.647z + 57.324 \\ A_o(z) &= z^2 - 1.823z + 0.837, \end{aligned}$$

where the bandwidth of the polynomial A_o is $5Hz$.

The reference model for the servo control system is a 13th order FIR filter with a $31Hz$ bandwidth, windowed by the Hamming function. The bandwidth of the FIR filter is chosen in order to avoid the excitation of a known resonance of the slide around $40Hz$.

The X-Y positioning table contour described in [7] is used in order

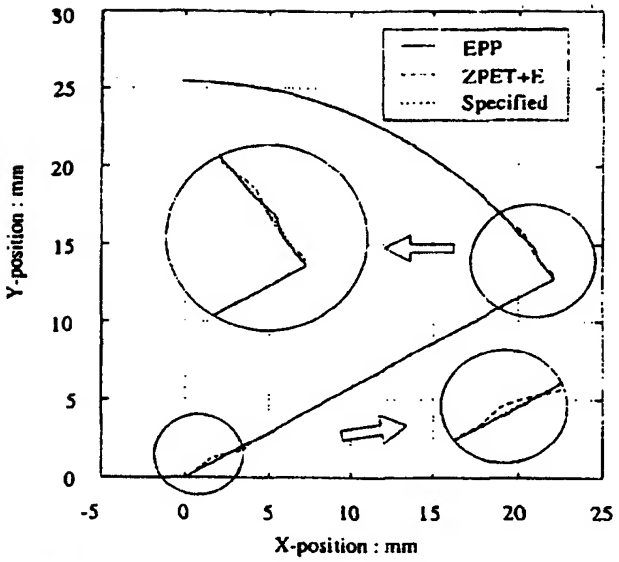

Figure 2: Contouring experiments with the ZPET+E-filter and the EPP methods

to verify the tracking accuracy of the EPP method. The contour consists of a straight line of $25.4mm$ raising 30° from the X-axis, immediately followed by a circular arc with a radius of $25.4mm$, extending 60° to the Y-axis (figure 2).

The performance of the EPP controller is compared with the performance of a controller designed by the E-ZPET method [7]. Figure 3 shows the resulting reference models for both methods. Both transfer functions exhibit unit gain in the low frequency region, but the bandwidth of the E-ZPET controller, which cannot

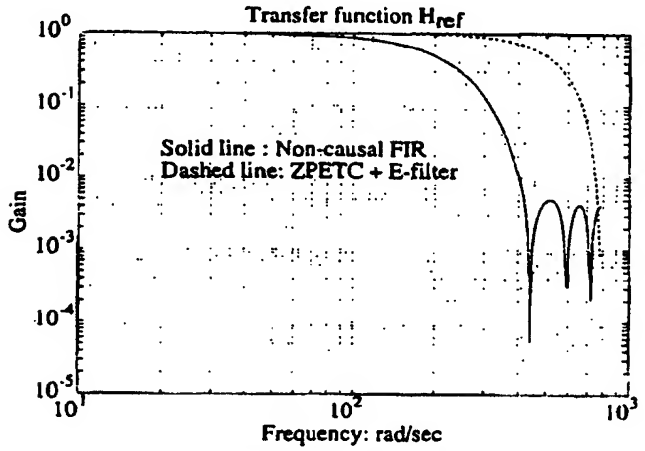

Figure 3: Frequency responses of $H_{ref}(z)$ for the E-filter enhanced ZPET method and the EPP method

be specified and extends to 100 Hz, while the bandwidth of the EPP method extends to $25Hz$ (which is about the closed-loop bandwidth).

The large transient errors at the starting and the cornering points of the contour (figure 2) indicate the over-compensation of the E-ZPET algorithm. The EPP controller gives lower overall tracking errors (figure 4) than the other controller due to the direct inclusion of $B_{MP}^{-}(z)$ in the feedforward function $T(z)$ (Eq. 9) in order to give a more accurate approximation of the inverse closed-loop transfer function.

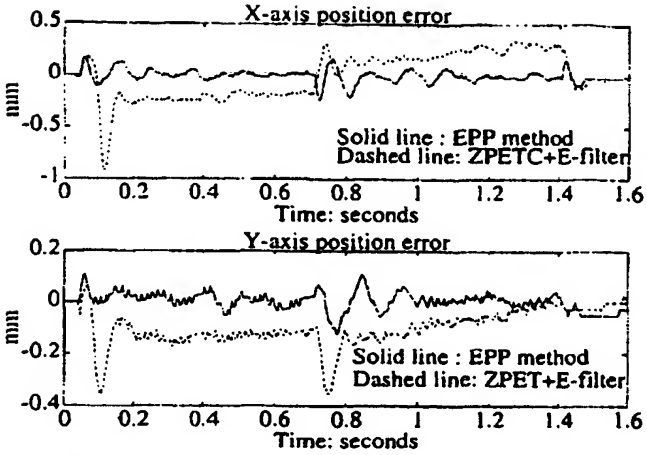

Figure 4: Position error for the ZPET+E-filter and the EPP methods

3 Feedback controller design with disturbance observer

Unaccounted external disturbances and modelling errors are rather rule than exception in motion control applications. Coulomb friction and stiction forces always exist in mechanical interfaces like bearings, so do cutting forces in machine tools during metal removal operations. Modelling errors stem either from an incomplete model or from varying loads on the controlled system. If these disturbances and errors are not accounted for in the feedback controller design, they give rise to tracking errors during contouring and nonzero steady-state errors during positioning.

Since the 40's, integral control has been the *de facto* approach to remove steady- state errors in most controller designs. Although its wide acceptance in practice, one persistent problem with integral control is its adverse effect on servo performance and robustness. For high-performance motion control applications, it is necessary to find a replacement for integral control which retains robustness and performance while enhancing disturbance rejection. The use of a disturbance observer is proposed here as a valuable alternative.

The idea behind the disturbance observer is to detect external disturbances acting on a controlled system by comparing the predicted outputs from a system model with the measured outputs. A high-quality disturbance observer design should satisfy following requirements:(i) be applicable to multiple-output measurement systems, to take advantage of the multiple sensors to give more reliable estimations of the disturbance; (ii) provide a methodology to find the observer gains which can preserve both performance and robustness of the closed-loop system.

3.1 Formulation of the disturbance observer

Consider a single-input-multiple-output system represented by its discrete state space model:

$$\begin{cases} x_{k+1} &= \Phi x_k + \Gamma u_k + \Gamma d_k \\ y_k &= C x_k + \nu_k, \end{cases} \tag{10}$$

with measured outputs y_k. The process disturbance d_k enters the system together with the control input u_k. To model the dynamic behavior of the expected disturbance, we presume that the external disturbance is generated by a stochastic dynamic process described by

$$d_{k+1} = \Phi_d \cdot d_k + w_{d,k}, \tag{11}$$

which is excited by white noise $w_{d,k}$. Both systems can be merged to form an augmented system

$$\begin{Bmatrix} x \\ d \end{Bmatrix}_{k-1} = \begin{bmatrix} \Phi & \Gamma \\ 0 & \Phi_d \end{bmatrix} \begin{Bmatrix} x \\ d \end{Bmatrix}_k + \begin{Bmatrix} \Gamma \\ 0 \end{Bmatrix} u_k + \begin{Bmatrix} 0 \\ w_d \end{Bmatrix}_k,$$

$$y_k = \lfloor C, 0 \rfloor \begin{Bmatrix} x \\ d \end{Bmatrix}_k \tag{12}$$

The augmented system is controlled by a linear feedback controller

$$u_k = -K\hat{x}_k - \hat{d}_k,$$

with feedback gain K, and an additional term $\hat{d}_k$ to compensate external disturbance d_k. $\hat{x}_k$ and $\hat{d}_k$ are the estimated state and disturbance. The observer for the state and disturbance has the standard observer structure.

Having decided the structure of the controller, one question we are immediately confronted with is to choose the gain values K for the feedback control and the gains for the state and disturbance observer which can meet our requirements on disturbance rejection and robustness to model parameter variations. Most literature suggests the pole placement method for the controller and observer design. However, this approach often leads to very poor robustness [5]. Therefore it would be preferrable if we could find the observer gain which does not incur robustness loss in the closed-loop system. This can be achieved with the so called loop transfer recovery (LTR) method.

The LQG/LTR method was formulated in an attempt to regain the excellent stability margins associated with LQ regulators that are lost when a Kalman filter is introduced in the LQG-formulation. It is only one of several alternative methods, like H_∞-, H_2- and μ-synthesis [5], but it has the advantage of guaranteeing excellent robustness.

To obtain a balanced design between robustness and performance, Doyle and Stein developed an adjustment procedure to tune the observer dynamics which is always stable and will gradually recover the loop transfer function of LQ-control (which is known to be more robust than the LQG-design).

The LTR procedure assumes a Kalman filter structure for the observer, then adds a fictitious disturbance vector $\tilde{w}$ to the plant in the form

$$\tilde{w} = r\Gamma, \tag{13}$$

with covariance

$$R_{\tilde{w}} \equiv E\{\tilde{w} \cdot \tilde{w}^T\} = r^2 \Gamma^T \Gamma, \tag{14}$$

where r is a real number. Outputs y are assumed to be subject to noise ν with intensity $R_\nu \equiv E\{\nu \cdot \nu^T\}$. By gradually increasing the intensity of the fictitious disturbance toward infinity, $r \to \infty$, the loop transfer function of the associated LQG controller will converge to that of the LQ controller.

Before applying the LTR method to the disturbance observer design, we reformulate the extended system in Eq. 12 and add the fictitious disturbance $\tilde{w} \equiv \Gamma \cdot r$ needed in the LTR procedure to give

$$\begin{Bmatrix} x \\ d \end{Bmatrix}_{k+1} = \begin{bmatrix} \Phi & \Gamma \\ 0 & \Phi_d \end{bmatrix} \begin{Bmatrix} x \\ d \end{Bmatrix}_k + \begin{Bmatrix} \Gamma \\ 0 \end{Bmatrix} u_k + \begin{bmatrix} \Gamma & 0 \\ 0 & 1 \end{bmatrix} \begin{Bmatrix} r \\ w_d \end{Bmatrix}_k$$

$$y_k = \lfloor C, 0 \rfloor \begin{Bmatrix} x \\ d \end{Bmatrix}_k + \nu_k, \tag{15}$$

where $R_{w_d} \equiv E\{w_d \cdot w_d^T\}$ is the intensity of external disturbance w_d yet to be determined. The covariance of the measurement noise can be obtained from the sensor resolution with a presumed probability density function such as the Gaussian distribution.

Since it can be shown that the disturbance observer gain does not affect the resulting controller's poles, we may first apply the LTR procedure to the original system model (Eq. 10) without the disturbance state d_k and increase the intensity of the fictitious process disturbance Γr to drive the state observer poles to converge. With the obtained intensity r_∞, we apply the LTR procedure again to the extended system in Eq. 15 and gradually increase disturbance intensity w_d as long as the maximum singular value $\bar{\sigma}(T(\omega))$ does not increase significantly beyond the closed-loop bandwidth. Since we assume that maximum singular value $\bar{\sigma}(T)$ has been determined by the allowable variation $\bar{\sigma}(\Delta)$ in the feedback design stage, it should not be further reduced, especially at frequencies beyond the closed-loop bandwidth.

3.2 Experimental verification

To verify the disturbance observer scheme, the same machine tool slide mentioned above for feedforward control experiments is used here again. The slide system has a discrete-time state-space model

$$\begin{Bmatrix} p \\ v \end{Bmatrix}_{k+1} = \underbrace{\begin{bmatrix} 1.0 & 0.0526 \\ 0.0 & 0.8842 \end{bmatrix}}_{\Phi} \underbrace{\begin{Bmatrix} p \\ v \end{Bmatrix}_k}_{x} + \underbrace{\begin{Bmatrix} 0.0018 \\ 0.0637 \end{Bmatrix}}_{\Gamma} u_k$$

$$y_k = \underbrace{\lfloor 1 \;\; 0 \rfloor}_{C} \begin{Bmatrix} p \\ v \end{Bmatrix}_k \tag{16}$$

identified at 250 Hz sampling frequency.

Using the LQ-method to find the state feedback gain K, we formulate the objective function J:

$$J = \sum_{k=0}^{\infty} (p_k^2 + \rho u_k^2) \tag{17}$$

that includes the output position and the control input weighted by a positive number ρ. The constant feedback gain K which minimizes the objective function J satisfies an algebraic *Riccati* equation. The resultant poles of the closed-loop system are the n roots within the unit circle of the $2n$ th-order dynamic system

$$\rho + H(z^{-1}) \cdot H(z) = 0,$$

where $H(z)$ is the transfer function matrix from input u to position output p. The closed-loop poles shift from the open-loop poles toward the zeros as the control weight ρ decreases. The damping ratio of the resultant closed-loop system is greater than 0.7 as long as the closed-loop bandwidth is less 50 Hz. Therefore, it is not necessary to include the velocity v as penalty in the objective function to increase the damping ratio of the closed-loop system.

The discrete-time LQ controller has a finite gain margin β between

$$\frac{1}{1+\sqrt{\frac{\rho}{R}}} \le \beta \le \frac{1}{1-\sqrt{\frac{\rho}{R}}},$$

for uncertainty in the control input matrix $\beta \cdot \Gamma$ [2]. For the slide, the gain margin β of the closed-loop system reduces as the bandwidth of the closed-loop system increases. We choose a closed-loop bandwidth of 21.7 Hz with feedback gains $K = \lfloor 56.63, 8.21 \rfloor$ in order to retain a sufficient gain margin $\beta = [0.58, 3.59]$, or equivalently
$[-4.72, 11.11]$ dB, in the control matrix.

Although all states of the slide table system are directly measured, we still use the Kalman filter to estimate the velocity, the position and the external disturbance in order to attenuate measurement noises and compensate for the disturbance.

The measurement noise for position ν_p and that for velocity ν_v are assumed to be uncorrelated, and their respective variance values: $R_{\nu,v}$ for velocity and $R_{\nu,p}$ for position measurement noises are

assumed to be 1/24 and 1,

$$R_\nu \equiv \begin{bmatrix} R_{\nu,p} & 0 \\ 0 & R_{\nu,v} \end{bmatrix} = \begin{bmatrix} \frac{1}{24} & 0 \\ 0 & 1 \end{bmatrix}.$$

The variance of position measurement noise $R_{\nu,p}$ is based on a uniform probability density function which is centered at the encoder reading and extends midway to the adjacent readings; the variance of the velocity measurement $R_{\nu,v}$ is purposely increased to account for the voltage ripples in the tachometer output and its multi-stage conversion (tachogenerator → attenuating amplifier → A/D converter). However, only their ratio is important to the Kalman filter design.

Two disturbance variances are yet to be assigned before applying the LTR technique: one for the fictitious disturbance with the same input matrix, i.e. $\tilde{w} \equiv r\Gamma$, the other with a presumed constant R_{w_d} to represent the undetermined intensity of the external disturbance.

We apply the LTR technique to the state-space model first without disturbance dynamics to find the limiting magnitude of the fictitious disturbance $R_{\tilde{w}}$ that makes the resulting loop transfer function from the system input u_k to the controller output $\tilde{u}_k = -K\hat{x}_k$ gradually converge to that of the full state feedback system from system input u to controller output $\tilde{u}_k = -Kx_k$, which means the loop transfer function of LQG control is recovered to that of the LQ control.

With the obtained intensity $R_{\tilde{w},\infty} = 10^6$, we iterate with increasing disturbance intensity R_{w_d} and monitor its maximum singular value $\bar{\sigma}(T)$ to find the maximum value of R_{w_d} which does not reduce the gain margin $\bar{\sigma}(\Delta)$ of the resultant closed-loop system significantly. In order to preserve enough robustness margin, intensity of the external disturbance is selected to be 2×10^3 which hardly decreases the maximum singular value $\bar{\sigma}(\Delta(z))$ at frequencies above 20Hz. The resultant gain for the observer corresponds to observer poles at 0.00, 0.759, and 0.956 for position, velocity, and disturbance respectively. This pole pattern is quite different from that of the Butterworth filter.

To verify the performance of the disturbance observer, a trajectory consisting of a smooth $9th$-order spline [16] is tracked by this disturbance-compensated LQG controller. The peak velocity of the motion profile reaches $220\,mm/sec$ at the middle of the trajectory where the motor reverses its torque direction. The same trajectory is also tracked by an integral LQG controller with the same feedback gain for comparison. The integral gain $k_i = 0.9$ is obtained by tuning the integral control gain to give the least tracking errors with little oscillation after the slide reaching the final position. Both controllers use the same feedforward algorithm and the same feedback gains.

Tracking errors and controller output for both controllers are illustrated in **figure 5** and **figure 6**, respectively. As shown in **figure 6**, the input voltage to the servomotor almost reaches the maximum output voltage ($50\,volts$) of the amplifier. From experiments we performed to identify the system model, the system model deviates significantly from the real system behavior in this output region. However, even at high tracking velocity the disturbance-compensated LQG control shows no oscillations in its controller output and the final position after reaching the desired position (**figure 6** and **figure 5**). The disturbance-compensated controller also gives smaller overall errors than the integral LQG control.

Comparing the estimated disturbance and the output of the integrator, the amplitude of the integral output is much larger than that of the estimated disturbance due to the fast accumulation of the output errors at high-velocity tracking. A larger integral output can easily saturate the actuator and cause numerical overflow

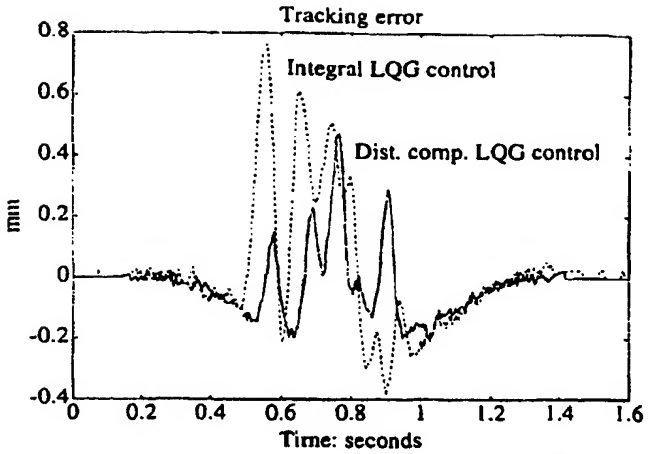

Figure 5: Tracking errors of the disturbance-compensated LQG control and of the integral LQG control during the tracking experiments

in the digital processor. Usually, the integrator requires a longer word-length storage [2] in fixed-pointed controllers to avoid overflow and special precautions to avoid saturation and terminal oscillations in practical implementations. However, the disturbance observer can be directly implemented in the controller without any modification, and the estimated disturbance can be a useful information for system diagnostics. For example, the estimated disturbance in the cutting tool feedrate controller for machine tools can indicate the cutting force. Excessive cutting force, or sudden drop in the cutting force may indicate a worn, or broken tool.

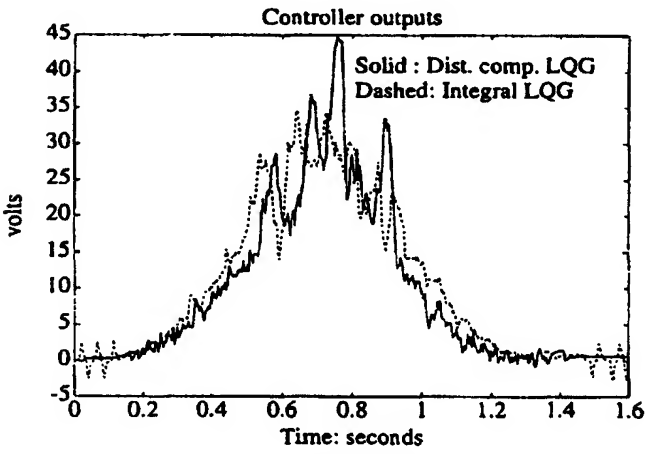

Figure 6: Outputs of the integral LQG and the disturbance-compensated LQG controller during the tracking experiments of the slide

4 Global control scheme

The feedforward signal u_f is added to the input of the closed-loop system to compensate for the non-zero reference input command y_{ref}. Consequently, the feedback controller only has to take care of the deviations from a zero-input response. This scheme can only work when the estimated state $\hat{x}$ is also reduced to a zero-input-state. This can be done by subtracting from $\hat{x}$ the so-called reference state x_{ref} which occurs due to the reference input y_{ref}. The reference state could be generated by a model with an

observer-like structure [3] as

$$\begin{cases} x_{m,k+1} &= \Phi x_{ref,k} + \Gamma u_{f,k} \\ x_{ref,k} &= x_{m,k} + L_{ref}\,[y_{ref,k} - C x_{m,k}] \end{cases} \tag{18}$$

to ensure that the resulting reference state vector x_{ref} is compatible with reference output y_{ref} and no difference at the steady state.

Observer gain L_{ref} is obtained by assuming measurement noise ν_{ref} and process disturbance $w_{ref} = \Gamma w_{ref}$ and applying the Kalman filter design method to the following model :

$$\begin{cases} x_{m,k+1} &= \Phi x_{m,k} + \Gamma u_{f,k} + \Gamma w_{ref,k} \\ y_{ref,k} &= C x_{m,k} + \nu_{ref,k} \end{cases} \tag{19}$$

The variance of ν_{ref} represents the round-off errors in computation. The process disturbance w represents the errors in u_f resulting from the inexact inverse feedforward transfer function (Eq. 9). However, only their relative values can affect the resultant Kalman filter gain. Although we are free to select a high gain L_{ref} to keep the reference states closely following the desired output, but to avoid generating reference states difficult to track or exciting unmodelled resonances, we should select the observer poles around the closed-loop bandwidth.

The three parts of the controler: feedforward, feedback and reference state generator can now be assembled together in a powerful general control scheme shown in **figure 7**.

5 Conclusion

By combining a noncausal filter in the feedforward path in an extended pole placement method with the use of a disturbance observer in the feedback path, a high performance motion control

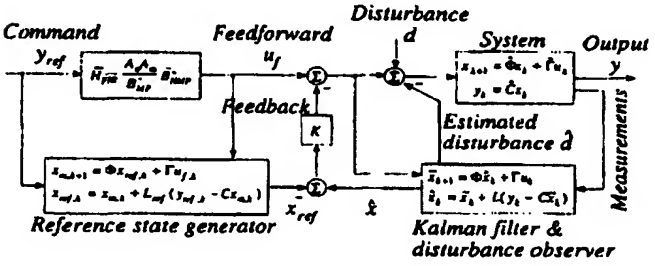

Figure 7: General control scheme

design system is obtained leading to minimal tracking errors, maximal robustness against model errors and external disturbances and, very important, a selectable bandwidth of the closed-loop system, enabling to avoid excitation of unmodelled resonances.

Acknowledgement

This text presents research results of the Belgian Programme on Interuniversity Poles of Attraction initiated by the Belgian State, Prime Minister's Office, Science Policy Programming. The scientific responsibility is assumed by its authors.

6 References

[1] Åström, K.J., Hagander, P., and Sternby, J., 1984, Zeros of sampled systems, Automatica, 20(1):31-38.

[2] Åström, K.J. and Wittenmark, B., 1984, Computer Controlled Systems, Prentice-Hall, Inc., Englewood Cliffs, N.J., U.S.A.

[3] Bengtsson, G., 1973, A theory for control of linear multivariable systems, Technical Report 7341, Division of Automatic Control, Lund Institute of Technology, Sweden.

[4] Clark, D. W., Mohtadi, C., and Tuffs, P., 1987, Generalized Predictive Control - Part I. the basic algorithm, Automatica, 23(2):137-148.

[5] Doyle, J.C. and Stein, G., 1979, Robustness with observers, IEEE Transactions on Automatic Control, AC-24(4):607-611.

[6] Franklin, G.F., Powell, J.D., and Workman, M.L., 1990, Digital Control of Dynamic Systems, Addison-Wesley Publishing Company, Massachusetts, U.S.A., second edition.

[7] Haack, B. and Tomizuka, M., 1991, The effect of adding zeros to feedforward controllers, Transactions of the ASME, Journal of Dynamic Systems, Measurement, and Control, 113:6-10.

[8] IEEE Acoustics, Speech, and Signal processing Society, Digital Signal Processing Committee, editor, 1979, Programs for Digital Signal Processing, IEEE press, New York, U.S.A.

[9] Koren, Y. and Lo, C.C., 1991, Variable-gain cross-coupling controller for contouring, Annals of the CIRP, volume 40, pages 371-374.

[10] Miu, D.K., 1991, Physical interpretation of transfer function zeros for simple control systems with mechanical flexibilities, Transactions of the ASME, Journal of Dynamic Systems, Measurement, and Control, 113:419-424.

[11] Safonov, M.G. and Athans, M., 1977, Gain and phase margin of multiloop LQG regulators, IEEE Transactions of Automatic Control, AC-22:173.

[12] Taylor, F.J., 1983, Digital Filter Design Handbook, Marcel Dekker, Inc., New York, U.S.A.

[13] Tomizuka, M., Dornfield, D., Bian, X.-Q., and Cai, H.-G., 1984, Experimental evaluation of the preview servo scheme for a two-axis positioning system, Transactions of the ASME, Journal of Dynamic Systems, Measurements, and Control, 106:1-5.

[14] Tomizuka, M., 1987, Zero phase error tracking algorithm for digital control, Transactions of the ASME, Journal of Dynamic Systems, Measurement, and Control, 109:65-68.

[15] Torfs, D., De Schutter, J., and Swevers, J., 1992, Extended bandwidth zero phase error tracking control of nonminimal phase systems, Transactions of the ASME, Journal of Dynamic Systems, Measurement, and Control, 114:347-351.

[16] Van Aken, L., 1987, Robot Motions in Free Space : Task Specification and Trajectory Planning, PhD thesis, Mechanical Engineering Department, Katholieke Universiteit Leuven, Belgium.